第 34 卷第 1 期 无 机 化 学 学 报 Vol.34 No.1
2018 年 1 月 CHINESE JOURNAL OF INORGANIC CHEMISTRY 11-19

基于非贵金属镍的金属有机大环的光解水放氢性能

李和川 李明凤 何 成* 段春迎
(大连理工大学精细化工重点实验室,大连 116024)

摘要:将具有 NN(氮氮)双齿配位点的席夫碱配体 L2(L2=1,4-苯二-2′-吡啶腙)与镍构筑得到一例[2+2]型金属有机大环$[Ni_2(L2)_2(CH_3CN)_4](ClO_4)_4\cdot 4CH_3CN$ (**2**),并将其用于可见光条件下的光解水产氢研究。该非贵金属光催化体系由催化剂、光敏剂(荧光素,Fl)和电子牺牲剂(三乙胺)三部分组成。相比于具有相同配位环境的单核配合物$[Ni(L1)_2(CH_3CN)_2](ClO_4)_2$(**1**,L1=3-甲酰基苯-2′-吡啶腙),金属有机大环 **2** 作为催化剂具有较高的光催化活性,其产氢 TON 值可以达到 3 100 $mol_{H_2}\cdot mol_{cat}^{-1}$,归因于荧光素分子可能与金属有机大环 **2** 形成超分子配合物,提高了光致电子转移效率。

关键词:金属有机大环;镍;光催化产氢;超分子
中图分类号:O614.81+3 **文献标识码**:A **文章编号**:1001-4861(2018)01-0011-09
DOI:10.11862/CJIC.2018.017

Construction of a Noble-Metal-Free Nickel Metal-Organic Macrocycle for Photocatalytic Hydrogen Production

LI He-Chuan LI Ming-Feng HE Cheng* DUAN Chun-Ying
(*State Key Laboratory of Fine Chemicals, Dalian University of Technology, Dalian, Liaoning* 116024, *China*)

Abstract: A nickel based metal-organic macrocycle $[Ni_2(L2)_2(CH_3CN)_4](ClO_4)_4\cdot 4CH_3CN$ (**2**) constructed from bidentate Schiff base ligand L2 (L2=1,4-benzenedicarboxaldehyde-bis(2′-pyridinylhydrazone)) with multiple N atoms was utilized to produce hydrogen through splitting of water by visible light (λ>400 nm). This noble-metal-free photocatalytic system consists of a catalyst, photosensitizer (fluorescein, Fl) and sacrificial electron donor (Triethylamine, NEt_3). Using the metal-organic macrocycle **2** as a proton reduction catalyst, the activity of the photocatalytic system is high, with a turnover number (TON) of approximately 3 100 $mol_{H_2}\cdot mol_{cat}^{-1}$. In contrast to the metal-organic macrocycle **2**, a mononuclear complex $[Ni(L1)_2(CH_3CN)_2](ClO_4)_2$ (**1**, L1=3-formyl benzaldehyde-2′-pyridylhydrazone) with similar coordination environment has a low efficiency on producing hydrogen. The enhanced efficiency of the catalyst **2** is likely ascribed to the formation of supramolecular complex between fluorescein and the macrocycle which enhances the efficiency of photoinduced electron transfer. CCDC: 1576598, **1**; 1576599, **2**.

Keywords: metal-organic macrocycle; nickel; light driven H_2 production; supramolecular

0 Introduction

The splitting of water through artificial photosynthesis (AP) is a key transformation towards the conversion of solar energy into stored chemical potential in the form of fuel[1-2]. For water splitting, the reductive side of the reaction involves the light-driven conversion of aqueous protons into H_2. Currently, the

收稿日期:2017-09-28。收修改稿日期:2017-10-18。
国家自然科学基金(No.21531001)资助项目。
*通信联系人。E-mail:hecheng@dlut.edu.cn

most prevalent strategy for proton reduction consists of a three component system[3]. These systems typically consist of a catalyst, photosensitizer (PS), and a sacrificial electron donor[4-5]. Recent studies on noble-metal-based[6-13] and noble-metal-free[14-16] homogeneous systems for light-driven hydrogen production have shown high activity. However, significant problems in the noble-metal-free molecular systems include relatively low catalyst turnover numbers for hydrogen formation. Besides, most of the systems based on organic dyes suffer from a reduction quenching step which produces unstable PS^- which reduces the stability of the system[3]. With precise organization of the catalytic centers and organic ligands into a metal-organic macrocycle, remarkable performance in hydrogen formation can be realized. In addition, the cavities of macrocycles have a special physical and chemical environment, such as hydrophilic/hydrophobic properties, hydrogen bonding, π-π stacking interaction, electrostatic interaction and so on, which can interact with the photosensitizer forming a supramolecular complex to enhance the electron and energy transfer efficiency[17].

In 1922, Paul Sabatier reviewed the state of the art of catalysis in organic chemistry and highlighted the specific behavior of nickel catalysts[18]. Nickel, as an earth-abundant and relatively low-cost material, may be a worthwhile basis for proton reduction catalysts. DuBois and co-workers have also shown that mononuclear nickel(Ⅱ)-bis(diphosphine) complexes are effective catalysts for electrochemical hydrogen generation. While photocatalytic hydrogen generation from the nickel-phosphine complexes is long-lived, the activity of the photocatalytic system with the nickel phosphine catalyst is low, with a turnover frequency (TOF) of approximately 20 equivalents of H_2 per hour[19-21].

Schiff base ligands have received considerable attention as chelating ligands for transition metal catalysts. In this article, a new metal-organic macrocycle $[Ni_2(L2)_2(CH_3CN)_4](ClO_4)_4\cdot 4CH_3CN$ (**2**) was constructed using the ligand L2(L2=1,4-benzenedicarboxaldehyde-bis(2′-pyridinylhydrazone)) consisting of multiple N atoms and nickel ions (Scheme 1). Because

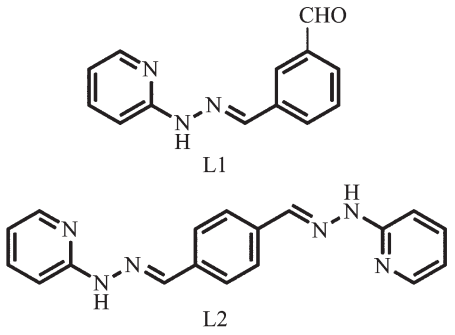

Scheme 1 Structures of ligands L1 and L2

the Ni(Ⅱ) of macrocycle **2** can be coordinated with the fluorescein (Fl) molecules to form supramolecular complex, the photocatalytic activity of catalyst **2** was higher than that of $[Ni(L1)_2(CH_3CN)_2](ClO_4)_2$ (**1**, L1=3-formyl benzaldehyde-2′-pyridylhydrazone) under similar reaction conditions. And the metal-organic macrocycle **2** significantly improves the stability of the catalytic system.

1 Experimental

1.1 Materials and physical measurements

All chemicals were of reagent grade quality obtained from commercial sources and used without further purification. The elemental analyses of C, H and N were performed on a Vario EL Ⅲ elemental analyzer. ^{1}H NMR spectra were measured on a Varian INOVA 400M spectrometer. ESI mass spectra were carried out on a HPLC-Q-Tof MS spectrometer. The fluorescent spectra were measured on a JASCO FP-6500.

Cyclic voltammetry measurements: Electrochemical measurements of catalysts **1** and **2** were performed in CH_3OH solutions with 0.1 $mol\cdot L^{-1}$ $TBAPF_6$ working on ZAHNER ENNIUM Electrochemical Workstation with a homemade Ag/AgCl electrode as a reference electrode, a platinum silk with 0.5 mm diameter as a counter electrode, and glassy carbon electrode as a working electrode. The addition of *p*-toluenesulfonic acid (0.1 $mol\cdot L^{-1}$ in CH_3OH) was carried out with syringe.

Fluorescence quenching experiments: A solution (2.0 mL) of Fl at 10 $\mu mol\cdot L^{-1}$ concentration in a CH_3OH /H_2O solution (1:1, *V*/*V*, pH=11.5) was prepared in a

quartz cuvette fitted with a septum cap, and the solution was degassed under N_2 for 15 min. Aliquots of 20 μL of the catalysts were added, and the intensity of the fluorescence was monitored by steady state fluorescence exciting at 460 nm on a Spex fluoromax-P fluorimeter with a photomultiplier tube detector.

Photocatalytic proton reduction experiments: Photoinduced hydrogen evolution was made in a 15 mL flask. Varying amounts of the catalysts **1** and **2**, Fl and NEt_3 in CH_3OH/H_2O (1∶1, *V*/*V*) were added to obtain a total volume of 5.0 mL. The flask was sealed with a septum and degassed by bubbling argon for 15 min. The pH of this solution was adjusted to a specific pH by adding HCl or NaOH and measured with a pH meter. After that, the samples were irradiated by a 500 W Xenon lamp with the 400nm light filter, and the reaction temperature was maintained at 293 K by using a thermostat water bath. The generated photo-product of H_2 was characterized by GC 7890T instrument analysis using a 5A molecular sieve column (0.6 m×3 mm), thermal conductivity detector, and argon used as carrier gas. The amount of hydrogen generated was determined by the external standard method.

1.2 Syntheses of L1 and L2

The ligand L1 was synthesized by refluxing a methanol solution (40 mL) containing of *m*-phthalaldehyde (6 mmol, 0.8 g) and 2-hydrazinopyridine (6 mmol, 0.65 g) for 8 h. Yield: 72%. Anal. Calcd. for $C_{13}H_{11}N_3O$(%): H, 4.92; C, 69.32; N, 18.66. Found(%): H, 4.96; C, 69.10; N, 18.74. ^{1}H NMR (DMSO-d_6, 400 MHz): δ 10.93 (s, 1H), 10.02 (s, 1H), 8.03 (d, 2H), 8.01 (s, 1H), 7.90 (s, 1H), 7.62 (t, 2H), 7.39 (t, 1H), 7.23 (d, 1H), 6.73 (t, 1H).

The synthesis of L2 was similar to that described for L1 with the corresponding terephthalaldehyde (3 mmol, 0.4 g). Yield: 70%. Anal. Calcd. for $C_{18}H_{16}N_6$ (%): H, 5.10; C, 68.34; N, 26.56. Found (%): H, 5.16; C, 68.44; N, 26.71. ^{1}H NMR (DMSO-d_6, 400 MHz): δ 10.93 (s, 2H), 8.12 (d, 2H), 8.03 (s, 2H), 7.68 (s, 4H), 7.65 (t, 2H), 7.27 (d, 2H), 6.78 (t, 2H).

1.3 Syntheses of complexes 1 and 2

The ligand L1 (0.2 mmol, 0.045 g) and $Ni(ClO_4)_2\cdot 6H_2O$ (0.1 mmol, 0.037 g) were dissolved in 20 mL acetonitrile. The solution was refluxed for 4 h, and then slowly evaporated at room temperature. The brown block crystals (complex **1**) were obtained in several days. Yield : 45%. ESI-MS *m*/*z*: $[2L1+Ni]^{2+}$, 254.060 7; $[2L1+Ni+ClO_4]^+$, 607.072 5. Anal. Calcd. for $NiC_{30}H_{28}Cl_2N_8O_{10}$(%): H, 3.57; C, 45.60; N, 14.18. Found(%): H, 3.60; C, 45.56; N, 14.24.

The synthesis of complex **2** was similar to that described for **1** with the ligand L2 (0.1 mmol, 0.032 g) and $Ni(ClO_4)_2\cdot 6H_2O$ (0.1 mmol, 0.037 g). After several days, yellow block crystals were obtained. Yield: 55%. ESI-MS *m*/*z*: $[2L2+2Ni+ClO_4-H]^{2+}$, 423.839 4; $[2L2+2Ni+2ClO_4]^{2+}$, 473.800 4; $[2L2+2Ni+2ClO_4-H]^+$, 946.611 5; $[2L2+2Ni+3ClO_4]^+$, 1 046.495 1. Anal. Calcd. for $Ni_2C_{52}H_{56}Cl_4N_{20}O_{16}$ (%): H, 3.82; C, 42.31; N, 18.98. Found (%): H, 3.87; C, 42.26; N, 19.02.

1.4 X-ray crystallography

The data were collected on a Bruker Smart APEX Ⅱ X-diffractometer equipped with graphite monochromated Mo *Kα* radiation (λ=0.071 073 nm) using the SMART and SAINT[22] programs at 296 K for complexes **1** and **2**. Final unit cell parameters were based on all observed reflections from integration of all frame data. The structures were solved in the space group by direct method and refined by the full-matrix least-squares using SHELXTL-97 fitting on F^2[23]. The crystal data and details of the structure refinement of complexes **1** and **2** are summarized in Table 1.

CCDC: 1576598, **1**; 1576599, **2**.

2 Results and discussion

2.1 Crystal structural description

Single-crystal structure representations for the complexes **1** and **2** are shown in Fig.1. In the crystal structure of complex **1**, the nickel coordination sphere is a distorted octahedron, consisting of two N atoms from 2-pyridinylhydrazone group of one Schiff base ligand L1, two N atoms from another ligand L1 and two N atoms from two acetonitrile molecules coordinated to the nickel. Similar to the complex **1**, in the crystal of complex **2**, each of the two metal centers was octahedrally coordinated by two N atoms from two acetonitrile molecules and four N atoms that equally

Table 1 Crystal data and structure refinements for complexes 1 and 2

Complex	1	2
Formula	$NiC_{30}H_{28}Cl_2N_8O_{10}$	$Ni_2C_{52}H_{56}Cl_4N_{20}O_{16}$
Formula weight	790.21	1476.39
Crystal system	Orthorhombic	Triclinic
Space group	*Pccn*	$P\bar{1}$
a / nm	0.752 3(1)	0.893 8(2)
b / nm	2.067 8(1)	1.025 9(2)
c / nm	2.172 1(1)	1.947 0(1)
α / (°)		82.816(4)
β / (°)		82.468(4)
γ / (°)		70.355(4)
V / nm^3	3.378 7(1)	1.660 4(1)
Z	4	1
D_c / (g·cm^{-3})	1.553	1.476
F(000)	1 624	760
Reflection collected	26 395	31 540
Unique reflection (R_{int})	9 886	9 893
Goodness-of-fit on F^2	1.088	0.998
Final *R* indices[a,b] [$I>2\sigma(I)$]	0.069 9	0.052 6
R indices[a,b] (all data)	0.087 9	0.068 8

[a] $R_1=\sum(|F_o|-|F_c|)/\sum|F_o|$; [b] $wR_2=[\sum w(|F_o|-|F_c|)^2/\sum wF_o^2]^{1/2}$.

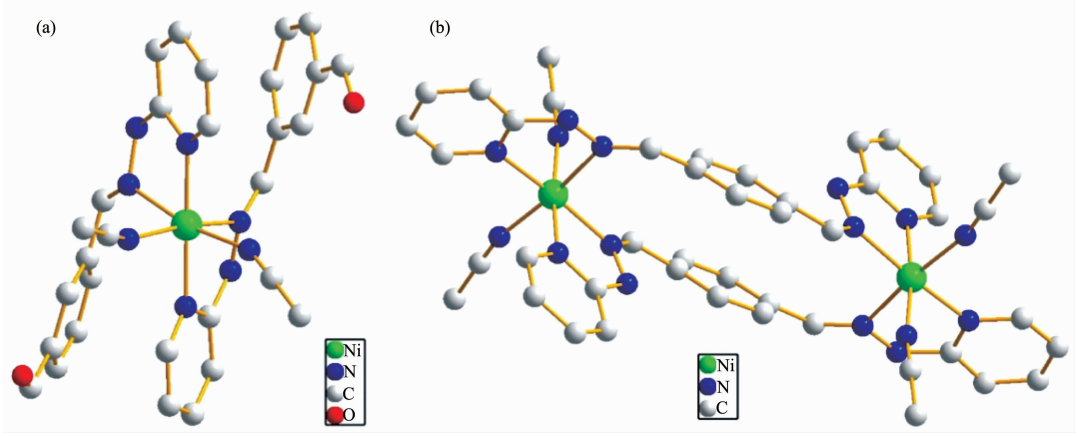

Anions and solvent molecules are omitted for clarity

Fig.1 Single-crystal structures of **1** (a) and **2** (b)

originated from one arm of the two ligands L2, respectively. As a result, the metal-organic macrocycle **2** was constructed by two ligands and two Ni(Ⅱ). In addition, these Ni(Ⅱ) centers feature an octahedral configuration that allows the production of free coordination sites by release of the acetonitrile molecules oriented outside of the metal-organic macrocycle. Moreover, the coordinated acetonitrile molecules were easily removed based on the configuration of **2**, producing the open sites of nickel for photosensitizer molecules. As a result, the photogenerated electron would be migrated from the photosensitizer to the catalyst during the photoreduction process, which was beneficial to achieving high activity in the catalytic system[24].

2.2 Cyclic voltammetry of the complexes

The cyclic voltammetry shows that the reduction potentials of Ni(Ⅱ)/Ni(Ⅰ) and Ni(Ⅰ)/Ni occur at −0.586

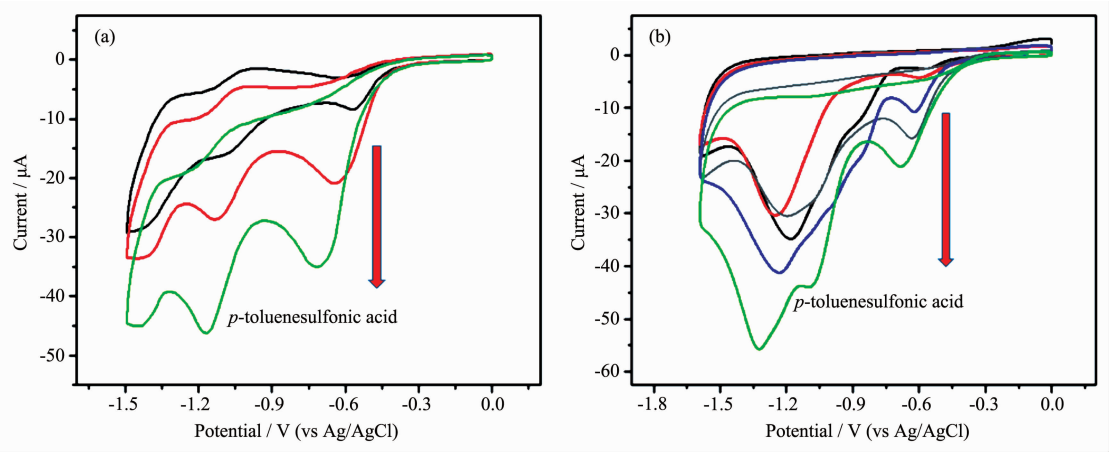

Scan rate: 100 mV·s^{-1}, c_1=1 mmol·L^{-1}, c_2=1 mmol·L^{-1}

Fig.2　Cyclic Voltammogram of **1** (a) and **2** (b) in CH_3OH with 0.1 mol·L^{-1} $TBAPF_6$ upon addition of *p*-toluenesulfonic acid with different concentrations

and −1.08 V (vs Ag/AgCl) respectively for **1** (Fig.2a). And the complex **2** exhibits the reduction processes of Ni(Ⅱ)/Ni(Ⅰ) and Ni(Ⅰ)/Ni at −0.595 and −1.28 V (vs Ag/AgCl), respectively (Fig.2b). In addtion, both the Ni(Ⅱ)/Ni(Ⅰ) potential for complexes **1** and **2** fall well within the range of that of proton reduction in aqueous media[25]. To investigate the role of the Ni complex as a proton reduction catalyst, cyclic voltammetry was performed in the presence of increasing amounts of *p*-toluenesulfonic acid. Addition of enough *p*-toluenesulfonic acid triggers the appearance of a new irreversible cathodic wave near the Ni(Ⅱ)/Ni(Ⅰ) response[26-27]. Increasing the concentration of *p*-toluenesulfonic acid raises the height of the new wave and shifts it to more negative potentials, indicating that complexes **1** and **2** are able to reduce protons through a catalysis process.

2.3　Complexes 1 and 2 as quenchers for the photosensitizer Fl

Complexes **1** and **2** can also serve as efficient quenchers for the photosensitizer fluorescein. The Stern-Volmer quenching constant K_{sv1} in this system was calculated as 3.217×10^3 L·mol^{-1} upon the addition of **1** into Fl solution in CH_3OH/H_2O (1∶1, *V*/*V*) as shown in Fig.3a. The quenching behavior can be considered as a photoinduced electron transfer process from excited state of Fl to **1**, providing possibilities for Fl to activate complex **1** for the production of H_2 in solution. The K_{sv1} for the catalyst **1** was higher than

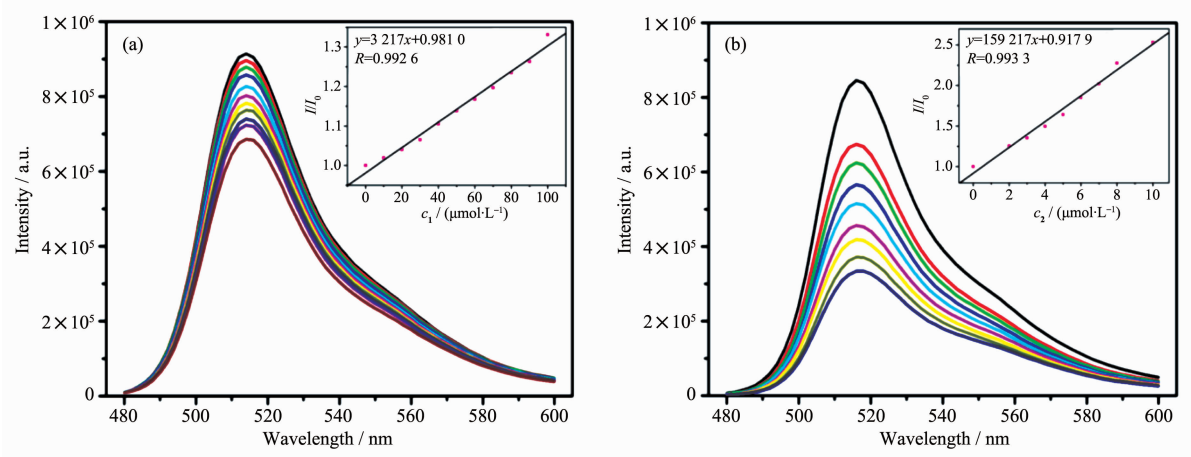

c_{Fl}=10 μmol·L^{-1}, V_{CH_3OH}:V_{H_2O}=1∶1; Inset: Stern-Volmer plot for the photoluminescence quenching of Fl by catalysts **1** (a) and **2** (b)

Fig.3　Emission spectra of fluorescein solutionin CH_3OH/H_2O solution upon addition of catalysts **1** (a) and **2** (b) with various concentration

the K_{sv3} reported for NEt_3 (0.44 $L \cdot mol^{-1}$). When the concentration of NEt_3 was 0.576 $mol \cdot L^{-1}$ (8%, *V*/*V*, the same below) and the concentration of catalyst **1** was 20 $\mu mol \cdot L^{-1}$ in the actual photocatalytic reactions, the $K_{sv3}c_{NEt_3}$ (0.25) is much higher than the $K_{sv1}c_1$ (0.06). Hence, a photoinduced electron transfer from the NEt_3 to Fl^*, with the unstable Fl^- is produced (reductive quenching), dominated the homogeneous photolysis of the reaction mixture instead of direct quenching by **1**. The Stern-Volmer quenching constant K_{sv2} of **2** (1.592×10^5 $L \cdot mol^{-1}$) is almost 50 times that of complex **1** (Fig. 3b). When the concentration of NEt_3 was 0.576 $mol \cdot L^{-1}$ (8%) and the concentration of catalyst **2** was 20 $\mu mol \cdot L^{-1}$ under photocatalytic conditions, the $K_{sv1}c_2$ (3.2) is much higher than the $K_{sv3}c_{NEt_3}$ (0.25). Hence, the quenching of the excited state of Fl by the catalyst **2** is largely dominated by the oxidative quenching. The initial photochemical step is the formation of Fl^+ through oxidative quenching by complex **2**[28-29]. It indicates that the metal-organic macrocycle **2** with a specific electronic transport pathway may be in favor of stabilizing the photosensitizer Fl compared with the mononuclear complex **1**.

2.4 Supramolecular complex formation between Fl and the macrocycle 2

Despite the cavity size of metal-organic macrocycle **2** being too small to encapsulate fluorescein molecules, the coordinated acetonitrile molecules were easily removed based on the configuration of **2**, which might produce open sites of nickel for photosensitizer molecules. To explore this hypothesis further, the ^1H NMR spectrum and ESI-MS spectrum of metal-organic macrocycle **2** in the presence of fluorescein were analyzed. The ESI-MS spectrum of **2** in CH_3OH exhibits a series of peaks at *m*/*z*=423.839 4, 473.800 4, 946.611 5 and 1 046.495 1 which are assigned to the $[2L2+2Ni+ClO_4-H]^{2+}$, $[2L2+2Ni+2ClO_4]^{2+}$, $[2L2+2Ni+2ClO_4-H]^+$, $[2L2+2Ni+3ClO_4]^+$ respectively, suggesting the formation and stability of the metal-organic macrocycle **2** in solution (Fig.4a). When an equimolar amount of Fl was added into the solution of **2**, two new intense peaks at *m*/*z*=590.192 1, 706.262 9 were

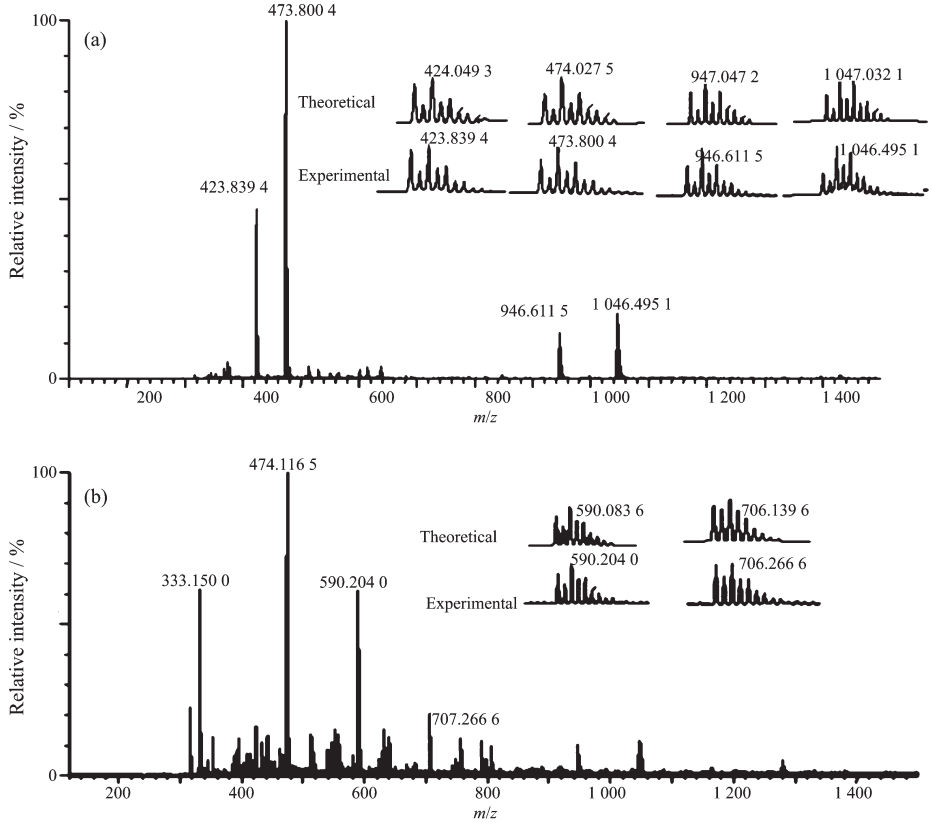

Fig.4 ESI-MS spectra of **2** in the absence (a) and presence (b) of Fl (1 equiv.) in CH_3OH

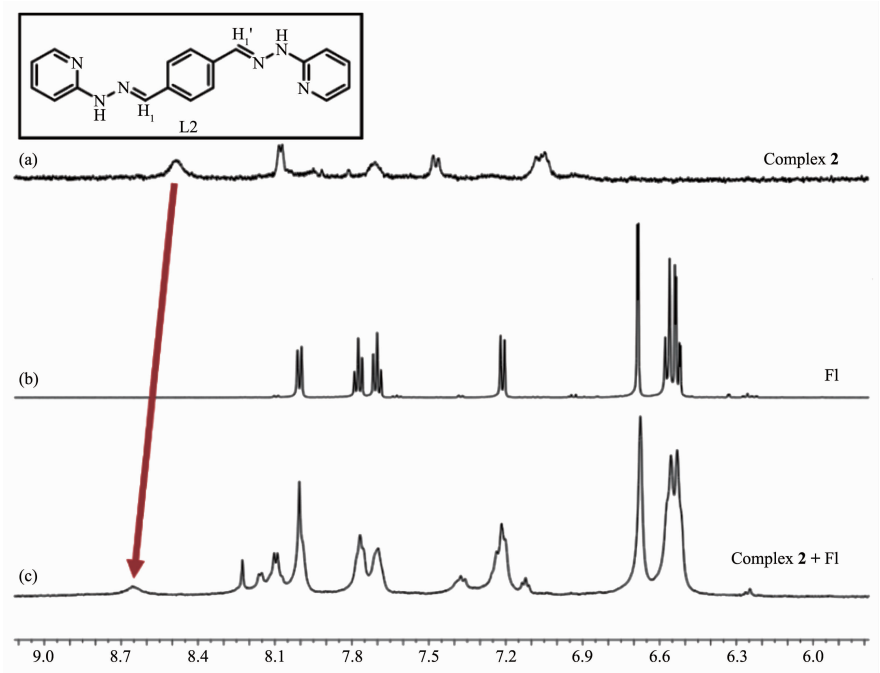

Inset: H_1 and H_1' in L2

Fig.5　^{1}H NMR spectra of **2** (a), Fl (b) and **2** in the presence of Fl (c)

observed (Fig.4b). A simple comparison with the simulation results based on natural isotopic abundances suggests that the peaks can be assigned to $[2L2+2Ni+ClO_4+Fl-H]^{2+}$ and $[2L2+2Ni+ClO_4+2Fl-H]^{2+}$, respectively. This result implies the formation of a 2:1 supramolecular adduct 2Fl·**2** in solution[30-31]. The ^{1}H NMR spectrum of **2** in the presence of Fl shows significant downfield shifts of the signals associated with protons H_1, H_1' nearby the Ni(Ⅱ) (δ=0.15) which suggested that the coordinated acetonitrile molecules were easily released for metal-organic macrocycle **2**, producing the free coordination sites of Ni(Ⅱ) centers for fluorescein molecules (Fig.5). Fl molecules are capable of coordinating to the Ni(Ⅱ) of macrocycle **2** and the Ni(Ⅱ) of mononuclear complex **1** is hardly coordinated with Fl on account of large steric hindrance, which well explains that the Stern-Volmer quenching constant of **2** (K_{sv2}=1.592×10^5 L·mol^{-1}) is almost 50 times that of complex **1** (K_{sv1}=3.217×10^3 L·mol^{-1}). Hence, macrocycle **2** could potentially be used for the construction of photocatalytic systems.

2.5　Catalytic behavior of the complex 2 in H_2 evolution

Proton reduction catalytic activity of complex **2** was evaluated with Fl as a photosensitizer (PS) and irradiation with visible light (λ>400 nm) in a CH_3OH/H_2O solvent mixture (1:1, *V*/*V*) containing NEt_3 at 25 ℃. The volume of H_2 was quantified at the end of the photolysis by gas chromatographic analysis[32-33]. The optimum pH value of the reaction mixture was maintained at 11.5, decreasing or increasing the pH value both resulted in a lower initial rate and shorter system lifetime for hydrogen evolution (Fig.6a). The decrease of the efficiency at higher pH values is likely due to the lower concentration of proton in solution[34]. It was found out that the optimal concentration of NEt_3 is 8% when fixing the pH of the system at the optimum value of 11.5 (Fig.6b). Furthermore, control experiments of the system with the absence of any one species of catalyst **2**, Fl or NEt_3 hardly yielded any observable amount of hydrogen, demonstrating that all of three species are essential for the hydrogen generation. This artificial photosynthetic system does not work well in the absence of the light either.

When the concentrations of Fl (3 mmol·L^{-1}) and NEt_3 (8%) were fixed, the volume of the hydrogen produced exhibited a linear relationship with the concentration of catalyst **2** in the range from 5 to 20

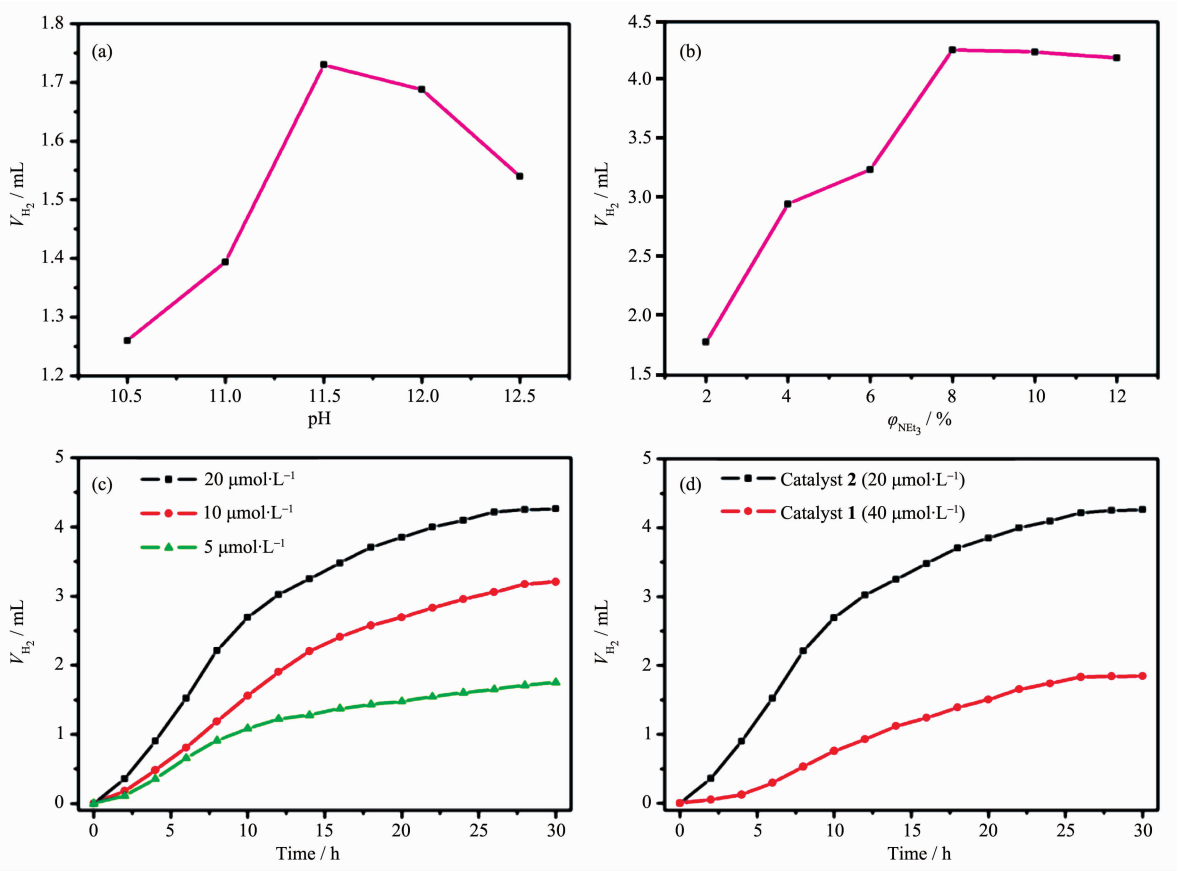

V_{CH_3OH}:V_{H_2O}= 1:1; (a) c_2=20 μmol·L^{-1}, c_{Fl}=3 mmol·L^{-1}, φ_{NEt_3}=10%; (b) pH=11.5, c_2=20 μmol·L^{-1}, c_{Fl}=3 mmol·L^{-1}; (c) pH=11.5, c_{Fl}=3 mmol·L^{-1}, φ_{NEt_3}=8%; (d) pH=11.5, c_{Fl}=3 mmol·L^{-1}, φ_{NEt_3}=8%

Fig.6 Initial rates of H_2 production in CH_3OH/H_2O of systems containing **2**, Fl and NEt_3 with different pH values (a) and systems containing **2**, Fl at pH 11.5 with different concentrations of NEt_3 (b); Photocatalytic hydrogen evolution of the systems containing Fl, NEt_3 with the concentration of **2** (c) and systems containing NEt_3, Fl in CH_3OH/H_2O upon addition with catalyst **1** or **2** (d)

μmol·L^{-1} (Fig.6c). When the concentration of catalyst **2** was at 5 μmol·L^{-1}, the system exhibited a high activity for a noble-metal-free system[14-16,19-21,35], achieving a turnover number of 3 100 mol_{H_2}·mol_{cat}^{-1} even after 30 h. At higher catalyst concentrations, even though a larger amount of H_2 is evolved, the TON does not scale linearly with catalyst concentration because of the limited lifetime of the system. In addition, when catalyst **2** (20 μmol·L^{-1}) was replaced by the mononuclear complex **1** (40 μmol·L^{-1}) which contains the same concentration of nickel ions in the same system consisting of Fl (3 mmol·L^{-1}), NEt_3 (8%), approximately only one third of hydrogen quantity of catalyst **2** was acquired (Fig.6d). The enhanced efficiency of the catalyst **2** is likely ascribed to the formation of supramolecular complex between fluorescein and the macrocycle which is beneficial to transfer electrons from the excited state of Fl to **2**.

3 Conclusions

In summary, a new strategy for constructing artificial photocatalytic systems to generate hydrogen from water by combining an organic photosensitizer with a redox active metal-organic macrocycle **2** was reported. Because fluorescein molecules are able to coordinate to the Ni(Ⅱ) of complex **2**, the photosensitizer and catalyst were forced close together, promoting the oxidative quenching of Fl by **2** when compared to the mononuclear complex **1**. This work may contribute to a bright future of supramolecular systems in

hydrogen evolution.

References:

[1] Lewis N S, Nocera D G. *Proc. Natl. Acad. Sci. USA*, **2006**, **103**:15729-15735

[2] Eisenberg R. *Science*, **2009**,**324**:44-45

[3] Han Z J, McNamara W R, Eum M S, et al. *Angew. Chem., Int. Ed.*, **2012**,**51**:1667-1670

[4] Bard A J, Fox M A. *Acc. Chem. Res.*, **1995**,**28**:141-145

[5] Esswein A J, Nocera D G. *Chem. Rev.*, **2007**,**107**:4022-4047

[6] Cline E D, Adamson S E, Bernhard S. *Inorg. Chem.*, **2008**, **47**:10378-10388

[7] Fihri A, Artero V, Razavet M. *Angew. Chem., Int. Ed.*, **2008**, **47**:564-567

[8] Du P W, Knowles K, Eisenberg R. *J. Am. Chem. Soc.*, **2008**, **130**:12576-12577

[9] Curtin P N, Tinker L L, Burgess C M, et al. *Inorg. Chem.*, **2009**,**48**:10498-10506

[10]Probst B, Rodenberg A, Guttentag M, et al. *Inorg. Chem.*, **2010**,**49**:6453-6460

[11]Streich D, Astuti Y, Orlandi M, et al. *Chem. Eur. J.*, **2010**, **16**:60-63

[12]White T A, Whitaker B N, Brewer K J. *J. Am. Chem. Soc.*, **2011**,**133**:15332-15334

[13]McNamara W R, Han Z J, Alperin P J, et al. *J. Am. Chem. Soc.*, **2011**,**133**:15368-15371

[14]Lazarides T, McCormick T, Du P W, et al. *J. Am. Chem. Soc.*, **2009**,**131**:9192-9194

[15]McCormick T M, Calitree B D, Orchard A, et al. *J. Am. Chem. Soc.*, **2010**,**132**:15480-15483

[16]Zhang P, Wang M, Dong J F, et al. *J. Phys. Chem. C*, **2010**, **114**:15868-15874

[17]Jing X, He C, Yang L L, et al. *J. Am. Chem. Soc.*, **2015**, **137**:3967-3974

[18]Ananikov V P. *ACS Catal.*, **2015**,**5**:1964-1971

[19]DuBois M R, DuBois D L. *Chem. Soc. Rev.*, **2009**,**38**:62-72

[20]DuBois M R, DuBois D L. *Acc. Chem. Res.*, **2009**,**42**:1974-1982

[21]Helm M L, Stewart M P, Bullock R M, et al. *Science*, **2011**, **333**:863-866

[22]*SMART*, *SAINT* and *XPREP*, Bruker Analytical Instruments Inc., Madison, WI, **1995**.

[23]Sheldrick G M. *SHELXS*-97, *Program for X-ray Crystal Structure Solution and Refinement*, University of Göttingen, Germany, **1997**.

[24]Stewart M P, Ho M H, Wiese S, et al. *J. Am. Chem. Soc.*, **2013**,**135**:6033-6046

[25]Artero V, Chavarot-Kerlidou M, Fontecave M. *Angew. Chem., Int. Ed.*, **2011**,**50**:7238-7266

[26]Razavet M, Artero V, Fontecave M. *Inorg. Chem.*, **2005**,**44**: 4786-4795

[27]Kasunadasa H I, Chang C J, Long J R. *Nature*, **2010**,**464**: 1329-1333

[28]Zhang P, Wang M, Dong J, et al. *J. Phys. Chem. C*, **2010**, **114**:15868-15874

[29]Li L, Duan L L, Wen F Y, et al. *Chem. Commun.*, **2012**,**48**: 988-990

[30]Yu H, He C, Jing X, et al. *Inorg. Chem. Front.*, **2016**,**3**: 1256-1263

[31]Yang L L, Jing X, He C, et al. *Chem. Eur. J.*, **2016**,**22**: 18107-18114

[32]Lazarides T, McCormick T, Du P W, et al. *J. Am. Chem. Soc.*, **2009**,**131**:9192-9194

[33]Zhang P, Wang M, Na Y, et al. *Dalton Trans.*, **2010**,**39**:1204-1206

[34]McNamara W R, Han Z, Alperin P J, et al. *J. Am. Chem. Soc.*, **2011**,**133**:15368-15371

[35]YANG Lin-Lin(杨林林), JING Xu (景旭), HE Cheng (何成), et al. *Chinese J. Inorg. Chem.*(无机化学学报), **2017**, **33**(6):913-922